

# Quantitative optical tomography of chemical waves and their organizing centers

A. T. Winfree,<sup>a)</sup> S. Caudle, G. Chen, P. McGuire, and Z. Szilagyi  
326 Biological Sciences West, University of Arizona, Tucson, Arizona 85721

(Received 31 October 1996; accepted for publication 4 November 1996)

Interference from topological, chemical and biological analogies led to the guess that a wide variety of homogeneous three-dimensional materials characterized by “excitability” might support persistent particle-like “organizing centers.” These are vortex filaments, typically rings, around which excitation fronts circulate in the uniform medium. Robust organizing centers were recently discovered numerically in several cases, motivating a search for them in nature. But if a candidate were observed there would still be no way to examine it for the expected topological intricacies. To solve this problem we designed and constructed a hybrid chemical/optical/computational instrument using the familiar principles of tomography by filtered backprojection. We demonstrate here that it can quantitatively resolve chemical vortex filaments in a new excitable medium fashioned for the purpose. The next step, not described here, is to use the light sensitivity of this medium to contrive initial conditions from which topologically exotic organizing centers would arise and possibly persist. © 1996 American Institute of Physics. [S1054-1500(96)01104-4]

**Heart muscle, nerves and some chemical media are “excitable”: they support travelling shock waves which leave a refractory wake close behind them. In one-dimensional media such waves resemble action potentials on nerve fibers. In two dimensions they resemble spiral waves radiating from electrical vortices on the surface of heart muscle. In three dimensions complex periodic travelling waves resembling scrolls radiate from vortex rings called “organizing centers.” Except for the simplest case (a rotationally symmetric vortex ring or fragments thereof) the topology, differential geometry, and complex dynamics of organizing centers have been described only in theory and in numerical experiments, not yet in heart muscle or in chemical media. Several years ago, we planned the first application of optical tomography to visualize organizing centers in transparent chemical media. Here we carry out that plan and improve upon it, demonstrating the feasibility of identifying whatever varieties of organizing center may persist in the new chemically excitable medium here described.**

## I. INTRODUCTION

Regenerative “excitability” dominates the dynamics of a wide variety of chemical, electrical, and physiological complex systems. Some of these are spatially extended, with adjacent elements connected by diffusion of ions, molecules, or electrical potential (e.g., calcium processes in the glial network of the brain and in single heart cells, cyclic AMP processes in developing slime molds, various isothermal reactions in chemical solutions, and action potentials in heart muscle). When not too small (length scale roughly  $\sqrt{[diffusion\ coefficient\ D \times excitation\ rise\ time\ T]}$ ), such volumes admit spatial patterning of their excitation, as in the

case of propagating action potentials and chemical waves. It has been suspected for half a century and known for half that time, that besides such rectilinearly translating solutions, there are stable vortex-like solutions of the equations of excitable media, characterized by an angular rather than a linear velocity. In a two-dimensional biochemical context these are seen in the laboratory as rotors, spinning out spiral waves that propagate away in all directions with period  $\approx 100T$ , entraining and phasing reactions throughout the entire medium. This dynamical mode organizes, for example, culmination and maturation of slime mold amoebae (spiral waves with five minute rotation period), periodic calcium release in cultured heart cells (1 s rotations within the single cell), and certain cardiac arrhythmias responsible for sudden cardiac death (10 rotations per second).

In three dimensions the analogous pattern of spatiotemporal organization is the “scroll wave,” whose axis of rotation is generically a closed ring (Winfree, 1974a). With no linking or knotting, these are typically rotationally symmetric, without torsion of the filament or twist of the surrounding concentration gradients. They were first discovered in (and remain until now the only organizing center confirmed in) chemically excitable media, where they shrink to enclose less area by  $2\pi D$  mm<sup>2</sup>/s and eventually vanish. They are mere transients. Their anatomy and dynamics for ten years have been extensively modeled numerically and analytically and quantitatively studied in the laboratory. (For a review and citations see Winfree, 1994a.) In particular numerical excitable media they are stable at a unique size, but this seems a rare case: generally they shrink and vanish, and they have no further interest for the purposes of this paper.

Scroll waves have since been demonstrated in the slime mold slug during development, in brain nuclei during spreading depression, and in heart muscle during potentially lethal tachycardias, but it remains difficult to go further with three-dimensional observations in any laboratory system. During

<sup>a)</sup>Electronic mail: art@cochise.biosci.arizona.edu

the past decade the most rapid advances of understanding came from computation, by solving the partial differential equations of local dynamics (whether chemical or electrical) and diffusive coupling in space (at  $D$  respectively  $1/1000$  to  $100 \text{ mm}^2/\text{s}$ ). Computationally it was found that scroll rings can be woven in complex textures. Given appropriate initial conditions, generously large rings come into being mutually entangled without topological linking or linked and knotted, apparently with arbitrary complexity. If care is taken with initial conditions and the parameters of local excitability, such beginnings evolve into a symmetric cluster of vortex rings like a three-dimensional gearbox. This compact particle-like “organizing center” radiates shock fronts at the period of the two-dimensional rotor while cruising and spinning through the (numerical) excitable medium  $\approx 100$  times slower than excitation propagates. It can be stable in the sense that deliberate perturbations, if not too large, merely deflect its course and rephase its rotation while it slowly rebounds to its original symmetric shape and resumes travel with the former speed and spin rate.

Is such stability generic? With less contrived parameters, does the typical “stable organizing center” prove to be merely an intricate initial condition that predictably comes unraveled until only shrinking and vanishing scroll rings remain? This can happen. But it also happens that some topological configurations persist as though their constituent vortex rings mutually repel and so can neither come unlinked nor shrink too small. Extensive computations with generic excitable media revealed a wide variety of persistent organizing centers made of various numbers of rings diversely linked and knotted (Winfree, 1994b, 1995). Notice “persistent” replaced “stable”: these objects squirm endlessly, never repeating a prior configuration, but forever preserving their topological invariants as foreseen in Winfree and Strogatz (1983a, 1983b, 1983c, 1984a, 1984b). Slices through their three-dimensional wave fronts look bafflingly complex, and the same picture is never seen again. This robustness suggests that if any natural stimuli create the initial conditions of such particles in laboratory excitable media, they should be observable, but they will be almost impossible to identify without capturing their complete three-dimensional anatomy for study. Welsh and Gomatam (1990) in fact present pictures of a writhing scroll ring in the traditional malonic acid excitable fluid, which they conjecture might be in transition from prior knotted or linked configuration like those shown in Winfree (1990). There is no way to know whether it really was knotted or linked, for want of a facility like hospital tomographic imaging tailored to the requirements of optics on this scale of size and duration.

## II. AN EXPERIMENTAL METHOD FOR OBSERVING ORGANIZING CENTERS

### A. A brief history

Computation has now ventured far beyond realities demonstrated in any laboratory system. To give reality a chance to catch up ATW planned a hybrid chemical/optical/computer instrument capable of capturing the spatial distri-

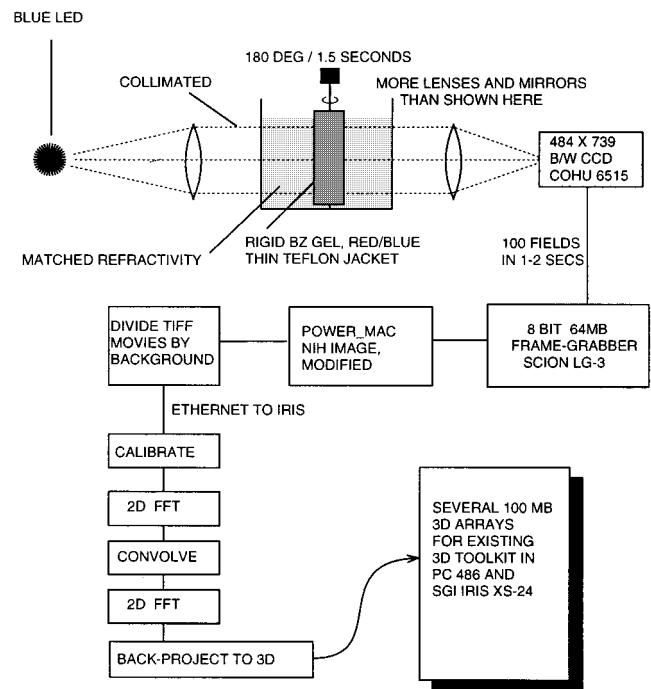


FIG. 1. Flow chart for tomographic observations, revised from Winfree (1992) flow chart by replacing glass cylinder with Teflon, replacing videotape with frame-grabber RAM, replacing malonic acid with cyclohexanedi-one, replacing tungsten/halogen source with LED, and dividing all frames by a background to remove faint circular scorings that make filament extraction unreliable.

bution of chemical species in a cubic centimeter of an excitable medium in which one might eventually conjure up persistent organizing centers. Referees approved the plan (most of its parts pretested), eager students enlisted, and this part of the project succeeded. Public-domain proposals on the laboratory web site were then supplemented by proven software and a tomographic volume capture of chemical concentrations, and this document was nucleated to describe the experimental method. A later report will presumably describe whatever organizing center dynamics it detects, after the coming effort to contrive appropriate initial conditions.

The instrument’s design and testing closely follow ATW’s abstract of the 1992 grant proposals for a workshop proceedings (Muller and Plessner, 1992) and for Santa Fe Institute lectures (Winfree, 1993), but with some important improvements (Fig. 1).

### B. A simple method of tomography

The aim of tomography is to infer the three-dimensional structure of a transparent object (in terms of optical density as a function of  $x$ ,  $y$ , and  $z$ ) from a series of projections through it. “Filtered backprojection” is an easy, nonmathematical way to do this. It is basically triangulation, and it is particularly simple in the case of parallel projections. Consider a single plane of such an object, consisting of a single small opaque particle in an otherwise perfectly transparent arena shown as an octagon in Fig. 2. Parallel beams of light

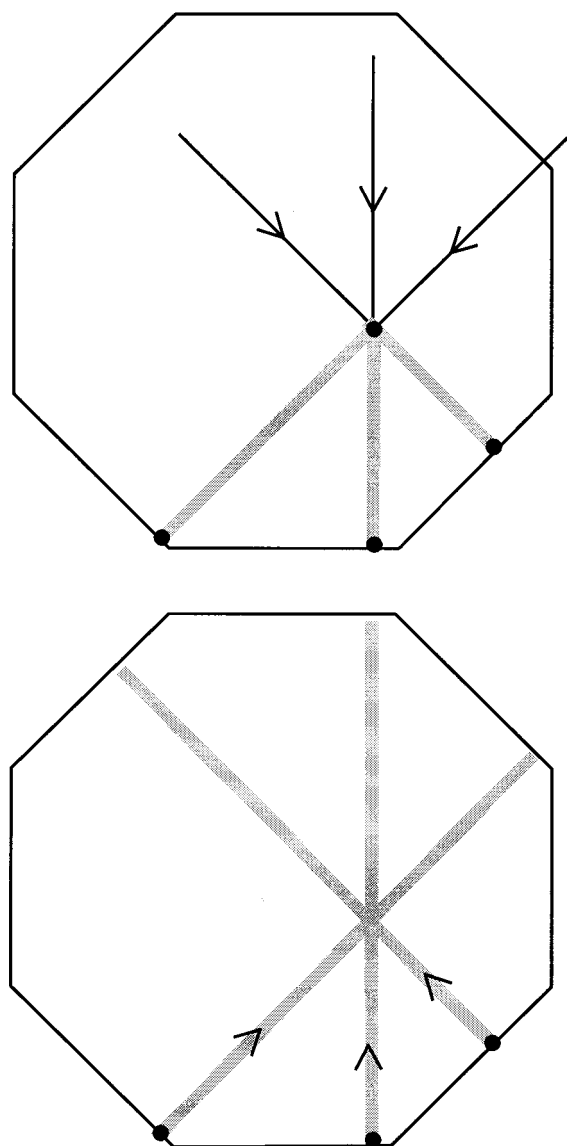


FIG. 2. The basic idea of tomographic backprojection, showing one horizontal plane in a three-dimensional transparent specimen. *Top*: a dense blob is projected from diverse angles onto “walls” (frames of a TIFF movie while the specimen rotates). *Bottom*: the blob is recreated by projecting those shadows back from the walls: the shadow is densest where all intersect.

from several directions (only three shown here) shadow the particle onto the arena walls as shown in the top panel. Now remove the particle and reverse the procedure: as in the bottom panel project the shadows from each wall back across the arena as a swath of light gray dust. The dust piles up at the unique site where all dust trails intersect, where the particle was. Do this for many directions and the localization improves. Do it for many particles simultaneously and the entire content of the arena is reconstructed from projections. This is the intuitive idea of backprojection, but there are wonderful refinements. For example, it is important to convolve each shadow with an empirically chosen filter function

before backprojecting (thus the name “filtered backprojection”). A place to begin reading is Chapter 9 of John Russ’s *Handbook of Image Processing* (1995).

### III. OPTICAL GIZMO

#### A. Light source

Initially, a 300 W tungsten-halogen filament provided illumination through a quartz cuvette of saturated aqueous copper sulfate and a pinhole at the focus of a 100 mm collimating biconvex achromatic doublet lens (see Gizmo Manual on <http://cochise.biosci.arizona.edu/~art>). However the backprojections in this paper were obtained with less trouble using instead several mA of dc current through a blue light-emitting diode sanded flat and masked by a 1/2 mm pinhole to provide a virtual point source of 450 nm light at the focal point of the collimating lens.

#### B. Light path

A 400 mm biconvex achromatic doublet lens decollimates and images the projection (through a third lens) onto the CCD camera. Long focal length is needed for depth of field and roughly parallel projection as assumed in our implementation of filtered backprojection. This long beam is reflected twice from 1/8 wavelength first-surface mirrors to keep the gizmo as compact as possible in a enclosure against dust.

#### C. Sample rotation and refraction

Our application of tomography is complicated (relative to comparable uses in medical imaging) by refraction. Because light propagates faster in the air than in our specimen (a refractive gel) it bends from the wanted straight parallel paths upon crossing each interface, depending on the interface angles. Fortunately, it does so uniformly because its speed (thus the refractive index) is independent of the chemical changes we seek to follow, i.e., independent of extinction coefficients or optical density.

Given a simple geometry, e.g., a cylinder of gel, the refraction geometry is predictable and could in principle be compensated numerically, but in practice this proves tricky. The simple key idea of 1992 was to evade the problem of diversely nonparallel projections by suspending the naked gel in a tank of liquid with identical refractive index. Then the only relevant interfaces become the glass–liquid interfaces. By placing them perpendicular to the light path all refraction is eliminated (supposing the gelled specimen is perfectly clear and uniform). Such a matching liquid might be the ungelled and uncatalyzed colorless reaction mixture or anything else if the gel is clothed in a thin impermeable jacket. Soft glass vials 0.1 mm thick proved troublesome: their refractive index (near 1.5) exceeds that of the gel (1.34) and matching liquid enough to distort the image more than we consider tolerable. However Teflon FEP (1.34–1.35) provides such a close match that even with 0.4 mm thickness the product of thickness by refractive index mismatch is much

less and pictures are correspondingly less distorted, especially near the edge of the projection (almost tangent to the cylinder wall).

Within the collimated beam the excitable medium is jacketed in a vertical Teflon cylinder rotating on the accurately vertical axis of a synchronous ac motor. Outside the Teflon cylinder the gel's refractive index is matched by a 7% aqueous sucrose solution (1.34), which also helps to dissipate the slight reaction heat and maintain a uniform temperature. This liquid is confined in a cuvette made of microscope slides perpendicular to the collimated beam.

By choice of motor a 360° rotation takes precisely 3 or 5 s: thus 4° or 2.4° per 1/30 s frame, or 2° or 1.2° per interlaced field capture. The Scion LG-3 frame grabber's 64 MB RAM fills in 4 s when 128 consecutive full frames have arrived at this rate, thus presenting 2 or 1 complete 180° scan of the gel. The replicate scan (if used) is inverted to present a stage of pattern evolution 1.5 s later, which we use (see below) to locate the vortex filament. From these full frames a region of interest centered on the rotation axle saves to a PowerMac hard disk in a few seconds, permitting fresh captures still later in evolution, from which we can assay filament motion under putative laws of dynamics (see below).

#### D. Image capture and resolution

The projected image is captured as alternating even/odd fields 60 times/s on a 640×480 pixel portion of the silicon charge-coupled device of a Cohu 6515 monochrome CCD camera with infrared filter. For focusing this is mounted on rack and pinion beyond the third lens (field lens, second imaging lens).

Two kinds of resolution need to be distinguished. In the projected blue images resolution is about as fine as wanted, depending only on choice of lenses and the CCD array. We typically use 29 pixels/mm in wide-field mode. By inserting the fourth ("magnifying") lens we realize severalfold greater magnification and resolution but in correspondingly smaller backprojected volume. Backprojected volumes are typically less well resolved, the nominal resolution being field width times  $\pi$ /number of projections. "Resolution" here refers to the central disk in Fourier space containing unattenuated harmonics corresponding to the longer spatial wavelengths. Shorter wavelengths outside this disk are unrepresented or underrepresented. Of course, if there are none (if the object is smooth) nothing is lost, so "resolution," though limited in this sense, is nonetheless perfect. As estimated in Winfree (1993, p. 280), backprojected resolution could exceed 1/10 of a 3 mm scroll wave spacing if 100 projections capture a 10 mm field at high resolution. In practice it looks much better, as determined by resolving an aviation fuel filter with pores 1/7 mm apart.

The problem of compromising backprojected spatial resolution (proportional to the number of projections captured) with temporal resolution (lost as wave fronts move between frames) was resolved by numerical simulation as reported in Winfree (1992) and (1993, p. 279). A spiral wave was continuously computed from the Oregonator reaction-

diffusion model while projecting numerically at intervals, then this slurred backprojection was evaluated: spiral waves rotating in 100 s were faithfully resolved by capturing 100 interlaced fields (50 frames) every few seconds.

It is critically important that the motor's rotation axis be aligned to the CCD array, and that the position of this axis on the captured projection be known precisely. Otherwise backprojections are grievously marred by geometrical artifacts. For example, single points become substantial circular arcs. Similarly, any nonuniformity of illumination (from the source, from dust on the CCD window, etc.) appears at the same position in every frame and so (consider Fig. 2) superposes in the volume a circular envelope of backprojection tangents concentric to the rotation axis. For examples of diverse tomographic artifacts see Russ (1995, Chap. 9).

#### E. Digitizing and pixel values

The captured frames are electronically processed in a Cohu 6500-series camera control unit, and then digitized at 8-bit depth. The calibration of such electronics tends to drift over time and as a function of temperature, resulting in non-linear departures from quantitative calibration in terms of ferroin micromoles/cm<sup>2</sup>. Unless the electronics are retuned as needed, a uniform field can also show vertical even/odd pixel stripes ("rainfall") in each projection. Though these largely vanish in the backprojection, they do interfere with numerical operations involving gradient derivatives (see below).

As published (Winfree, 1992, 1993) our prototype experiments involved capture to videotape and then transfer to a Data Translation digitizer under the control of public-domain NIH Image software (written by Wayne Rasband). This worked, but frame transfer through the Mac si NuBus was too slow. With the help of Tod Weinberg at Scion Corporation we modified Scion Corporation's adaptation of NIH Image to version 1.57 of 3/95 (<http://128.231.98.16/nih-image/>) so that it can save directly to 64 MB of RAM on the Scion LG-3 digitizer card at video rate (60 fields/s) in a PowerMac. This eliminates a number of errors and inconveniences involved in analog data storage and retrieval.

Image 1.57 was then extensively supplemented using Metrowerks Pascal in user.p with procedures for centering the rotation axle in the captured image, presenting captured TIFF movies for stereo viewing (by frame shifting a horizontally displaced copy to a later angle of rotation), background normalization, etc. Image software is used to scale pixel values so as to preserve their linear relation to the photon count, and inverted so 255=no light and 0=light-saturated for subsequent processing in C on a Silicon Graphics Iris. The entire TIFF movie is divided by a background frame to eliminate slight variations of "uniform" field intensity (dirt on cuvette window, etc.). Without this step the result is marred by faint cylindrical scorings which heavily interfere with numerical gradient calculations from the result, e.g., for locating the vortex filament. This division leaves only the extinction ratio, a function of integral absorption along the optical path to each pixel. These 8-bit pixel values are then converted (through an empirical fitting function similar to Beer's law)

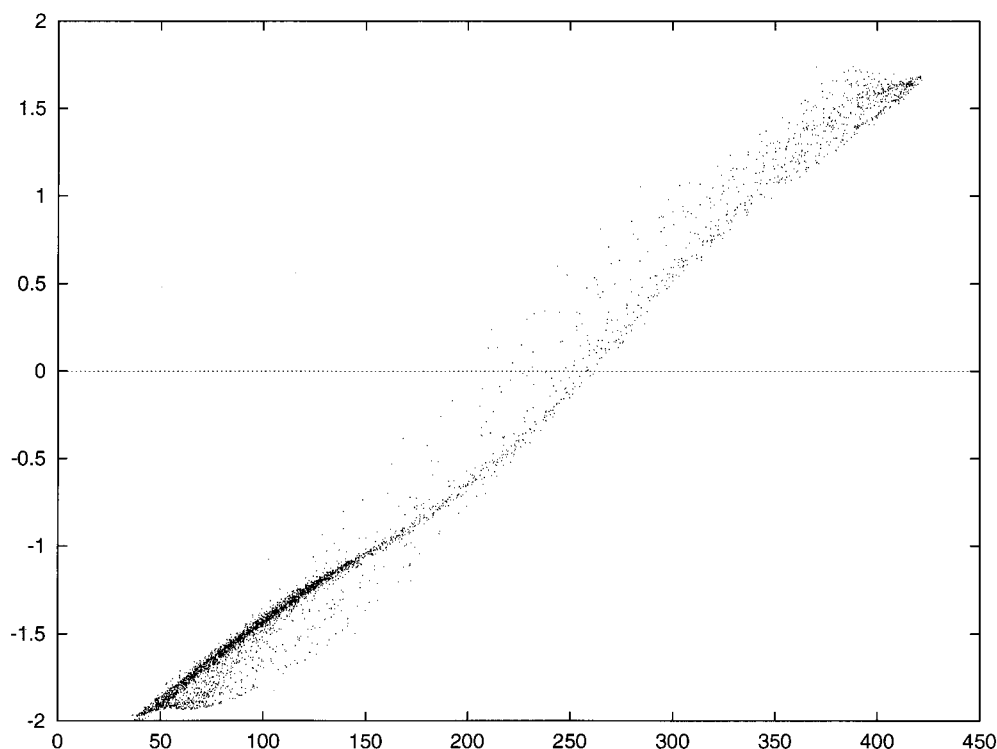


FIG. 3. In one  $45 \times 75$  pixel plane of a three-dimensional scroll wave obtained numerically from a partial differential equation, deviations of a chemical concentration from steady state are plotted vertically. Horizontally, reconstructed values in the backprojection should correspond one-to-one in monotone fashion, ideally linearly to the extent that filtered backprojection is quantitatively reliable (and reliably implemented) for chemistry, not just for geometry. Perfection is precluded by using only 45 projection angles and by some arbitrariness in tailoring the filter function  $(0.54 + 0.46 \cos \text{FREQ}) \times \text{FREQ}$  to attenuate high and low spatial frequencies. We judged that this 15/12/95 test came close enough to a straight line.

to calibrated micromoles/cm<sup>2</sup> of ferroin concentration. In the end the backprojected volume contains 8-bit integers proportional to ferroin micromolarity/cm<sup>3</sup>. Due to short period of re-excitation, their histogram peaks severalfold below the recipe's half micromole/cm<sup>3</sup> corresponding to red gel completely recovered from excitation.

## IV. DATA ANALYSIS

### A. Tomography

Alternate planes of each frame belong to two successive fields  $2^\circ$  or  $1.2^\circ$  apart, due to the CCD camera's interlacing of even and odd sets of simultaneously captured horizontal lines (not scanned as in analog television). Independently in each horizontal plane of the projections, the numbers proceed through a maze of manipulations from the 8-bit projected pixel values representing integral extinction to the final 8-bit volume of ferroin concentrations. Every step was written in C and checked by a wide variety of control experiments with precisely known correct outcome. These included:

- (1) A "Greek temple" of parallel opaque cylindrical columns at known coordinates;
- (2) an opaque perfect sphere (4 mm ball bearing) embedded in the Teflon-jacketed refracting gel to check for distortions in any direction;

- (3) an asymmetric twisted wire to check for mirror inversion of axes;
- (4) a metal foil with 0.07 mm holes in a hexagonal array 0.14 mm apart to check three-dimensional resolution;
- (5) spaced mm-scale rectangular prisms of transparent neutral density filter of known  $xyz$  dimensions and opacity to check quantitative handling of superposed transparency;
- (6) the two-dimensional "phantom" in Fig. 4 of Russ (1995, Chap. 9) for projection and backprojection, plus display of intermediate steps for comparison with his Figs. 5 and 9, as a check against other people's software;
- (7) a volume  $u(x, y, z)$  from partial differential equation computation of a twisted scroll wave: numerically projected onto planes at 100 angles then backprojected for a plot of  $u_{\text{original}}$  versus  $u_{\text{reconstructed}}$  comparing before-and-after values point by point (Fig. 3).

This process uncovered subtle (and blatant) errors and converged to the 8000 lines of TOMO-GRAPH source code available in two versions (one portable, one tailored to the SGI Graphics Library) as \*.tar.gz on <http://cochise.biosci.arizona.edu/~art> and thoroughly documented therein. Its 14 programs are operated through UNIX script files in which options and parameters can be set and recorded. The output is 64-bit binary volume of doubles for further processing, and an 8-bit version for volume rendering (e.g., Figs. 4 and 5).

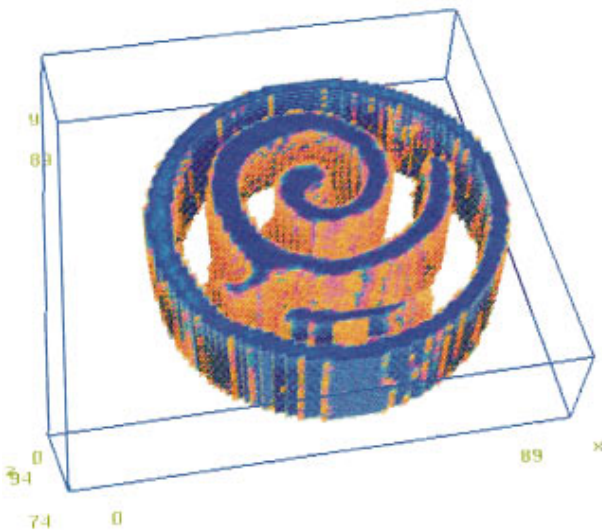


FIG. 4. A segment of our first really good reconstruction from cyclohexanedione. A scroll wave was created along the vertical  $z$  axis of a 9.3 mm Teflon cylinder, filmed during  $180^\circ$  of rotation, and backprojected on a large scale. Only 0.7 mm of the  $z$  axis is sliced out for presentation here, so that the inner coils of the scroll are not obstructed from view. The outside ring is the 0.4 mm thick Teflon jacket. Just inside this jacket lies a rind of invisibility believed to be due to imperfect removal of Teflon background absorption. Two full turns of a 2 mm scroll wave are visible inside that.

## B. Filament extraction

The further processing consists principally of identifying those voxels belonging to the nominal vortex filament. From there on, the data (integer triplets identifying filament cells) look the same to our differential geometry software as comparable data generated here since 1985 by solving the partial differential equations of reaction and diffusion to study vortex filament dynamics. Analogous to the experimental apparatus described here, we had built a FORTRAN toolkit for a succession of supercomputers. The output was two volumes of floating-point numbers, representing the two state variables (chemical concentrations or membrane potential and channel conductivity) of the excitable medium. Supplementary to this, the vortex filament was extracted for further processing in a PASCAL toolkit to assay the filament's curvature, torsion, etc., and the twist of concentration fields along it. These were related to its quantified motion by comparing consecutive filament images during the ongoing PDE evolution (e.g., in Henze and Winfree, 1991). Here we only demonstrate extraction of the filament in the same format but from tomographic backprojections (Fig. 5 bottom). Given the filament, much of the prior analysis can be repeated in this real-world context.

There is one important difference between solving PDE's and observing real chemical reactions: our tomographic method reveals only one chemical concentration, that of the blue-absorbing species, ferriin. In principle, a second dye could be used to probe a different feature of the chemical environment with a different color light, but at present we have only one. Filament detection in the past has used two independent state variables (commonly called  $u$  for unob-

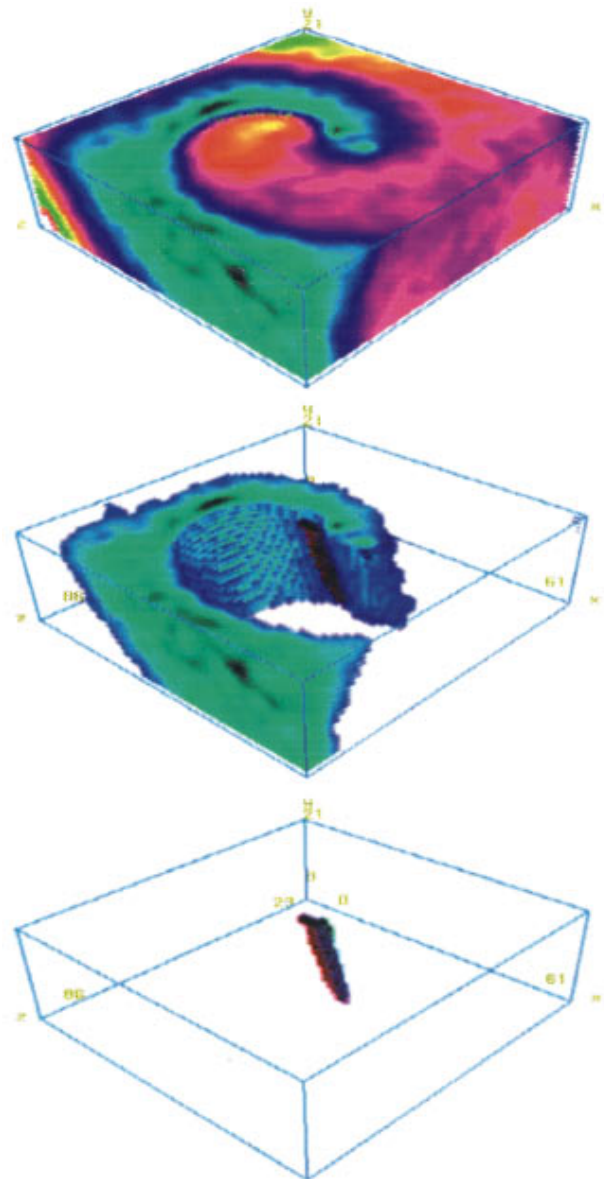


FIG. 5. This figure presents a 1 mm by 3.5 mm by 3.5 mm chunk out of a 30 mm long 9.3 mm-diameter cylinder of cyclohexanedione gel. Within this chunk, lying across the cylinder axis ( $z$ , horizontal here), a 4.5 mm long scroll wave is horizontally embedded among more complicated wave patterns. Viewing from the nominal top of the container one sees only parallel curves radiating alternately left and right from a source curve, and serial sections (not shown here) also present an uninformative spectacle. But viewed from the right perspective within the cylinder's depth, the scroll anatomy stands out. The top panel shows backprojected ferriin concentrations on the surfaces of this conceptually isolated chunk, colored roughly as in the original with high ferriin/low ferriin in reds, low ferriin/high ferriin in blues. The first half turn of a spiral wave appears on the top surface. The middle panel isolates the blue part, the oxidized propagating region, from its red background. Just inside the tip of this spiral (the inner edge of this scroll) the black region depicts the scroll axis as evaluated from the cross product of ferriin gradients taken at all voxels 1.5 s apart. This 1 mm long segment of the 4.5 mm filament is isolated in the bottom panel.

servable, e.g., bromous acid, and  $v$  for visible, e.g., ferriin). Their isoconcentration contours cross near the tip of the spiral wave, thus defining the vortex filament. The first method for numerical filament detection (Winfree, 1974b) used their

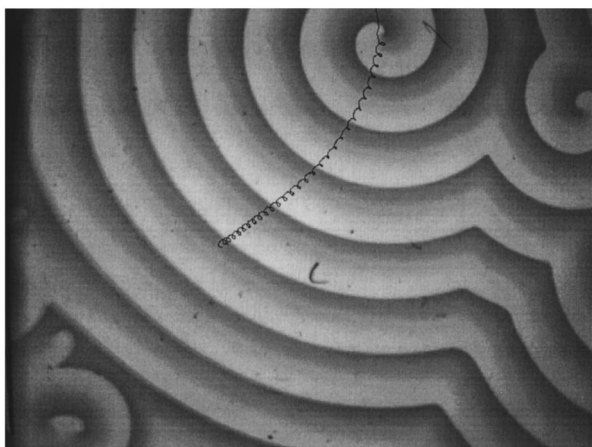


FIG. 6. This 25/10/95 snapshot of a thin layer of cyclohexanedione excitable reagent (1/3 more acid and four times more ferroin than above) was recorded by green panelescent background illumination. It shows two rotors, one of which was targeted for on-line continuous identification by the criterion that (visible) ferroin concentration gradient cross (invisible) bromous acid concentration gradient exceeds a threshold magnitude. Bromous acid concentration  $u$  was guessed qualitatively by solving the second equation of the Oregonator model with input from ferroin  $v$  observations (Winfree, 1992, 1993 p. 281, 1994a p. 48):  $u(x,y) = d/dt v(x,y) + v(x,y) - D \text{Laplacian } v(x,y)$ .  $d/dt$  was estimated from the difference of successive ferroin observations at 5 s intervals, and the Laplacian by summing the differences between neighboring pixels at one time. The superposed fine black curlique is the path of the spiral tip upward and rightward during the prior hour. Done in many planes from tomographic backprojections, this would be one slice in the path of the filament.

gradient vectors: they are large and conspicuously nonparallel only in the vortex core, so the magnitude of their three-dimensional vector cross product identifies the core, and its direction orients the filament.

There is a method (Winfree, 1993, 1994a) for inferring  $u$  from observed  $v$  and its time derivative, if the reaction kinetics from  $v$  is known, as approximated for example in the Oregonator model or the better Russian alternative (Aliev and Rovinsky, 1992). Figure 6 shows a single plane of cyclohexanedione excitable medium (see below) containing a rotor whose tip is automatically identified by observing  $v$ , estimating  $u$  by solving the reaction-diffusion equation, and then locating the pixels with maximum cross product of  $u$  and  $v$  gradients. The movement of this cluster of pixels, followed over time in every plane, is the motion of the filament in three dimensions.

In Fig. 5 (bottom two panels) one snapshot of the filament is constructed from two consecutive backprojections by a simplified cross-product-of-gradients method. Instead of trusting the kinetic model (which was designed for malonic acid reactions, not cyclohexanedione) to evaluate actual bromous acid concentrations,  $v$  gradients are evaluated in successive volumes 1.5 s apart, then crossed. They are nearly parallel everywhere deep in the gel, except along the vortex filament where isoconcentration surfaces fold sharply: there the cross products are large. The whole filament (of which only 1 mm is shown here lest outer wave fronts obscure the inner tip) is about 4.5 mm long, a chord in the 9.3 mm

cylinder, and its diameter is about half the nominal vortex core diameter ( $2-3 \text{ mm wavelength}/\pi$ ).

This method, involving both time and space derivatives, amplifies fine-grained pixel noise, so we smooth the raw projection data and/or the volume beforehand. As shown, this cross-product-of-gradients criterion typically locates a region in the concavity behind the excitation front's tip, where Barkley (1992) found the source of meander in spiral waves.

## V. CHEMISTRY

Our initial subject for the visualizations reported here is the vortex filament in a chemically excitable isothermal aqueous solution evolved from the original Belousov-Zhabotinsky oscillating reaction. The purpose of this evolution was to eliminate diverse artifacts from familiar BZ arrangements, e.g., convection currents in the 3-D volume, growing  $\text{CO}_2$  bubbles, and parameter gradients, notably of temperature and of incoming oxygen or outgoing substrates. Surface chemical gradients are eliminated by jacketing the gelled reagent in impermeable transparent Teflon. The temperature gradient comes from released reaction heat (several calories/ml in typical recipes). It is minimized by rotating the reaction volume in a water bath and by using so little catalyst (about 1/2 mM ferroin) that free-energy release is quite slow. This is necessary also to keep optical density low enough for transmission of enough light through 1 cm thickness at the 450 nm wavelength of greatest extinction ratio (50 to 100) between blue ferroin and orange ferroin. To obtain a uniform convection-free medium free of gas bubbles we gel the traditional malonic acid BZ reagent *in situ* with silicic acid. The usual procedure of preparing virgin gel first then allowing BZ reagents to diffuse into it is unsuitable to tomography of samples as thick as 1 cm because it leaves parameter gradients which strongly alter filament motion. The necessary alkalinity for silica gelation is also incompatible with the necessary acidity of BZ reagent. This required a modification of BZ reagent to work well in an environment slightly more alkaline than used heretofore, and discovery of a catalyst (fluoride ions) by which to set the gel in such acidity (Winfree, 1992, 1993). This gel has refractive index near 1.35.

The backprojections shown here use an agar gel of slightly lower refractive index. When such gels were first attempted with malonic acid substrate they served only for short-time observations due to accumulation of carbon dioxide bubbles unless the reactants are made so dilute that excitability becomes marginal, for example, exhibiting no meander. In a tomographic context this is disastrous: the bubbles refract light and the agar extrudes from its narrow jacket of Teflon. Bubbles could be eliminated by replacing malonic acid by something else that oxidizes to acetic or formic acids, or to anything other than  $\text{CO}_2$ . ATW tried this a quarter-century ago by testing diverse beta-diketones, eventually settling on 1,3-cyclohexanedione as a random choice among catalogued 1,2- 1,3- and 1,4- variants, then on ethyl acetoacetate (Winfree, 1974a). Jessen *et al.* (1976 and subsequent personal correspondence) later improved this recipe by substituting tri-fluoro-acetyl acetate. But in batch

reaction these and all subsequent attempts perform poorly in respect to optical clarity (a fog of by-product oil droplets scatters light) and in terms of longevity in units of spiral rotation periods. Kurin-Csorgei *et al.* (1995) finally solved this problem by trying the overlooked 1,4-cyclohexanedione. We refined their recipe in two-dimensional tests until it was excitable without oscillating and made spiral waves, then in three dimensions until it made scroll rings of adequate longevity.

The recipe in terms of the aqueous stock solutions from which we construct any of the hundred or so published variants of the BZ reagent (Jahnke and Winfree, 1991):

- 1.5 ml sodium bromate (21.8 g in 10 ml: 1.42 M);
- 1.0 ml diluted sodium bromide (2.5 g in 100 ml: 0.24 M);
- 0.75 ml sulfuric acid (17.2 ml in 100 ml: 3.26 M);
- 3.0 ml 1,4-cyclohexanedione (10 g in 100 ml: 0.89 M);
- wait half an hour for bromine color to clear then add (in a glass, not a plastic vial) 0.25 ml 25 mM ferroun.

Mix well then add to 5.25 ml hot water containing 0.1 g low melting-temperature agarose, and using a syringe force through a 5  $\mu\text{m}$  filter. The composition is now 0.17 M bromate, 0.18 M sulfuric acid, 0.20 M CHD, and 1/2 mM ferroun. Depending on losses in filters this makes more than 10 ml, enough for about 15 cm of 9.3 mm cylindrical gels. It sets in about 15 min at room temperature, quicker if chilled. The rotor period at room temperature is 50–60 s, and the radiating spiral wave spacing is 2–3 mm.

Fortuitously, this reagent is also light sensitive, so we can initiate scroll filaments by appropriate illumination. (Adding ruthenium bipyridyl further enhances the photosensitivity.) Without light sensitivity, the only alternative in gel systems was to pour a uniform gel layer atop a previous pour in which a wave front had been stimulated: its edge along the interface between pours became the scroll filament (Winfree and Jahnke, 1989). This is unsuitable for contrivance of any but the simplest geometries (scroll rings with no twist), an area already exhaustively explored without tomography as mentioned above. With light sensitivity we induce such rings using a column of light to erase a disk from a wave front; in theory (Winfree, 1985) successive adjacent stimuli can induce topologically exotic rings.

## VI. DISCUSSION

This project evolved in a deliberately unusual way. The explicit aim from the beginning was to handcraft all software from C/UNIX commands and all optical devices from a ‘‘junk box’’ of cannibalized lenses, motors, and bulk materials. In this way we made sure that no principle or device has hidden peculiarities: every component and process is understood and adapted to its specific purpose. The project was consequently instructive and took a long time (1992–6). Since the start of construction on this device at a time when there was no technique for visualizing vortex filaments three-dimensionally, two other ways appeared. Pertsov *et al.* (1993), Vinson *et al.* (1993), and Mironov *et al.* (1996) adapted the three-dimensional projection method of Winfree

and Jahnke (1989) for circular vortex filaments to the case of arbitrary shapes which do not cross over themselves in projection. This method would have difficulties with entangled filaments which necessarily cross over one another in all projections, and it cannot reconstruct wave fronts [as needed, e.g., by Pagola and Vidal (1987)], but only the vortex filament. But it is simple and serviceable for the cases engaged to present time. Cross *et al.* (1995), Su *et al.* (1994), and Tzalmona *et al.* (1990) demonstrated the utility of magnetic resonance imaging with a manganese-catalyzed two-dimensional version of the BZ reagent. This may develop into a method useful in three dimensions, much like optical tomography.

Meanwhile we have established that arbitrary vortex filament geometry can be acquired tomographically from chemical experiments. Our first implementations of the original plan (Winfree, 1992, 1993) were thought to be quantitative but turned out to distort geometrically due to imperfect refractive index matching and use of a cylindrical glass jacket, and to distort chemically due to diverse transforms en route to voxel values putatively proportional to [ferroun]. Today’s revised arrangement still quantitatively reports only deviations from mean [ferroun], because in each plane (separately) very low spatial frequencies are removed by convolution with the filter function (see Fig. 3 caption). We can, of course, restore these from the unfiltered projections. But the nonzero low spatial frequencies are still attenuated. Absolute quantitation is better handled by algebraic reconstruction techniques than by filtered backprojection.

What use will theorists have for such observations? First of all, there is now a substantial volume of (often contradictory) theory about the motion of twisted vortex filaments in 3-D excitable media. For recent reviews see Winfree (1993 and 1994a). Little of this is testable due to a profusion of undetermined parameters, and much of the rest has been tested only to order of magnitude. Three distinct kinds of test can soon be made:

- (1) Test of the topological essentials predicted before there were numerical experiments (Winfree and Strogatz, 1983a, 1983b, 1983c, 1984a, 1984b; Tyson and Strogatz, 1991). Are the mutual linkages and knottedness of vortex filaments related as foreseen to the integral twist along each filament? Do filaments fuse and hybridize, or do they pass through one another (or resist such passage), and do the results in any case conform to the ‘‘understood’’ topological transmutation rules? They do in numerical experiments (Winfree, 1994b, 1995) but do they in the real world?
- (2) Tests of the various putative laws of motion of vortex filaments (Biktashev *et al.*, 1994; Tyson and Keener, 1994; Winfree, 1994a; Mikhailov, 1995) which partly determine the stability or instability and the periodicity (in s and in cm) of nontrivial organizing centers. Existing theory seems not to cover generic vortex filaments of the kind that can be reliably computed within a grid of manageable size. Such filaments have substantial curvature and twist and they are impacted by wave fronts from

other segments. Rather, existing theory is about transients (not stable periodic steady states) in barely twisted and barely curved (huge) isolated filaments which do not meander and evolve very slowly. But these remain beyond economical numerical investigation except in a computational mesh too coarse for believable quantitation. The chemically excitable “analog computer” may provide a usefully complementary perspective when chemical recipes are improved to last longer without substantial change of relevant parameters. Then existing mathematical theories can finally be tested.

- (3) Tests of the bottom line: Are there persistent organizing centers in three dimensions? They might not be “stable” in any simple sense, e.g., if, as seems generic in numerical models, they glide and tumble through the medium, their component filaments meander, and waves of twistiness circulate along the constituent rings [Winfree (1994b, 1995)]. But do they persist? Does any version of the BZ medium support persistent particle-like solutions even vaguely resembling those anticipated by theorists?

This general-purpose arrangement for three-dimensional capture of chemical patterns has another possible application. Since 1952 theoretical biologists and some experimentalists have vigorously pursued the idea of Alan Turing that biological pattern formation might be a consequence of the spatially unstable interplay of local reaction kinetics with local transport processes, notably molecular diffusion or its larger-scale equivalent in turbulent convection of cytoplasm. A malonic acid/chlorite/iodide reaction with a starch indicator provided the first laboratory Turing patterns (Boissonade *et al.*, 1994; Epstein and Showalter, 1996; Lee and Swinney, 1995; Lee *et al.*, 1994; Ouyang *et al.*, 1995, and references therein). Their three-dimensional aspect has been little explored, but now might be through optical tomography.

A third possible application concerns an experimental arrangement like those invented for Turing patterns, in which distinct chemical solutions diffuse in opposite directions through a separating membrane. Using vycor porous glass for the separator, Ouyang and Flesselles (1996), Li *et al.* (1996), Belmonte *et al.* (1996), and Belmonte and Flesselles (1996) have chemically checked numerical experiments concerning the dependence of two-dimensional rotor behavior upon the parameters of excitability. All their results are fascinating, both for their confirmations of principles heretofore illustrated only in computers, and for several qualitatively distinct departures from the consensus of all published two-dimensional numerical experiments and mathematical theory. Because diffusion in vycor glass is about 20 times slower than in water, that separator is effectively thick enough to harbor significant three-dimensional structure, and such structuring would seem to be imposed by the steep opposite gradients of the major reactants. Is this really a functionally two-dimensional experiment, or would these surprising new effects receive a more illuminating interpretation if they could be viewed three-dimensionally?

A fourth possible application concerns self-oscillatory materials which are not conventionally excitable, but are

subjected to regularly periodic influences (Winfree, 1993, p. 281; Coulet and Plaza, 1994). Suppose each small volume entrains, but the frequency and amplitude of periodic influence are such that its phase lag is only barely stable. Then a stimulus exceeding some threshold will upset the volume’s locally stable phase relation to this periodic influence: instead of reverting directly to the stable phase relation by the short path, it falls back along the long path, losing a full cycle. This is “regenerative excitability.” The phase slip presumably propagates much as in any more familiar excitable medium, leading to the expectation that vortex rings may exist in wide classes of material (e.g., chemical solutions) which exhibit no excitability in the absence of appropriate periodic stimulation (e.g., by light). Optical tomography might provide the means to observe such phenomena for the first time.

Finally, there is the original motivation of our involvement with reaction–diffusion excitability in BZ media: their surprisingly close analogy with the electrical reaction–diffusion processes that organize the periodic beating or arrhythmic paroxysms of the human heart. Suggestions arose that myocardium should exhibit electrical rotors two-dimensionally and vortex filaments three-dimensionally, that critically timed electrical stimuli of a certain strength would evoke them, and that their expected size and period might account for familiar but unexplained tachycardias. These notions were based largely on laboratory experience with (and simulation of) the more conveniently observable rotors of BZ media. These predictions were eventually confirmed in the laboratory (Winfree, 1989, 1994c). Human myocardium is thick enough to accommodate a few long vortex filaments lying within the heart wall. Their configuration and its evolution would be nearly impossible to observe with three-dimensional grids of implanted electrodes, or by optical methods due to scattering and opacity. It is our hope that observation of filament dynamics within analogous chemically excitable media (like Fig. 5 middle) together with their surface manifestations (like Fig. 5 top) will facilitate interpretation of observations restricted to the surfaces of the heart.

*Note added in proof.* In October during the preparation of this manuscript we became aware that D. Stock and S. C. Muller (1996) in *Physica D* **96**, 396–403 implemented our original plan for optical tomography of scroll waves: “The set-up that is realized in this work was outlined by A. T. Winfree.” See ATW abstract in Muller and Plesser (1992) and Fig. 1 caption here.

## ACKNOWLEDGMENTS

In April 1992 ATW submitted these ideas to the National Science Foundation’s and the American Chemical Society/Petroleum Research Foundation’s referees together with a request for support to try whether unforeseeable practical problems could be overcome. Both were generous. Scott Caudle and Zoltan Szilagyi are Petroleum Research Foundation undergraduate Scholars; Gang Chen is and Patrick McGuire and Dean Schulze were Petroleum Re-

search Foundation graduate Fellows. We thank Dean Schulze for insisting in 1994 that backprojection could be moved from CRAY FORTRAN to workstation C and for drafting the first version of C software, much of which is still in use. Mark Gallagher spent many hours over our watchmaker's lathe and perfected the first successful optical arrangements in 1994. Tod Weinberg of Scion Corporation consulted on our timing problems with PowerMac RAM and volunteered to modify Scion Image to version 1.57 for undelayed access to frame-grabber RAM, completed in March 1995. Richard Field (March 1974 personal communication) suggested the use of cyclohexanedione.

- Aliev, R. R. and Rovinsky, A. B. (1992). "Spiral waves in the homogeneous and inhomogeneous Belousov-Zhabotinsky reaction," *J. Phys. Chem.* **96**, 732–736.
- Barkley, D. (1992). "Linear stability analysis of rotating spiral waves in excitable media," *Phys. Lett.* **68**, 2090–2093.
- Belmonte, A., Ouyang, Q., and Flesselles, J.-M. (1996). "Experimental survey of spiral dynamics in the Belousov-Zhabotinsky reaction," *J. Phys. (Paris)* (in press).
- Belmonte, A. and Flesselles, J.-M. (1996). "Experimental determination of the dispersion relation for spiral waves," *Phys. Rev. Lett.* **77** 1174–1177.
- Biktashev, V. N., Holden, A. V., and Zhang, H. (1994). "Tension of the organizing filaments of scroll waves," *Philos. Trans. R. Soc. London Ser. A* **347**, 611–630.
- Boissonade, J., Dulos, E., and De Kepper, P. (1994). "Turing patterns: From myth to reality," in *Chemical Waves and Patterns*, edited by R. Kapral and K. Showalter (Kluwer, Dordrecht), pp. 221–268.
- Coulet, P. and Plaza F. (1994). "Excitable spiral waves in nematic liquid crystals," *Int. J. Bifurcation Chaos* **4**, 1173–1183.
- Cross, A., Armstrong, R. L., and Reid, A. (1995). "Contrast enhancement of magnetic resonance images of chemical waves in the Belousov-Zhabotinsky reaction," *J. Phys. Chem.* **99**, 16616–16621.
- Epstein, I. R. and Showalter, K. (1996). "Nonlinear chemical dynamics: Oscillations, patterns, and chaos," *J. Phys. Chem.* **100**, 13132–13147.
- Henze, C. and Winfree, A. T. (1991). "A stable knotted singularity in an excitable medium," *Int. J. Bifurcation Chaos* **1**, 891–922.
- Jahnke, W. and Winfree, A. T. (1991). "Recipes for Belousov-Zhabotinsky reagents," *J. Chem. Educ.* **68**, 320–324.
- Jessen, W., Busse, H., and Havsteen, B. (1976). "Chemical waves in the 2,4-pentanedione/potassium bromate system," *Chem. Int. Ed. Engl.* **15**, 689.
- Kurin-Csorgei, K., Szalai, I., and Koros, E. (1995). "The 1,4-cyclohexanedione-bromate oscillatory system II. Chemical waves," *React. Kinet. Catal. Lett.* **54**, 217–225.
- Lee, K. J., McCormick, W. D., and Swinney, H. L. (1994). "Experimental observation of self-replicating spots in a reaction-diffusion system," *Nature* **369**, 215–218.
- Lee, K. J. and Swinney, H. L. (1995). "Lamellar structure and self-replicating spots in a reaction-diffusion system," *Phys. Rev. E* **51**, 1899–1915.
- Li, G., Ouyang, Q., Petrov, V., and Swinney, H. L. (1996). "Transition from simple rotating chemical spirals to meandering and travelling spirals," *Phys. Rev. Lett.* (in press).
- Mikhailov, A. S. (1995). "Three-dimensional kinematics," *Chaos, Solitons, Fractals* **5**, 673–679.
- Mironov, S., Vinson, M., Mulvey, S., and Pertsov, A. (1996). "Destabilization of three-dimensional rotating chemical waves in an inhomogeneous BZ reaction," *J. Phys. Chem.* **100**, 1975–1983.
- S. C. Muller and T. Plesser (1992). *Spatio-temporal Organization in Non-equilibrium Systems* (Projekt-Verlag, Dortmund), pp. 270–273.
- Ouyang, Q., Li, R., Li, G., and Swinney, H. L. (1995). "Dependence of Turing pattern wavelength on diffusion rate," *J. Phys. Chem.* **102**, 2551–2555.
- Ouyang, Q., and Flesselles, J.-M. (1996). "Transition from spirals to defect turbulence," *Nature* **379**, 143–146.
- Pagola, A. and Vidal, C. (1987). "Wave profile and speed near the core of a target pattern, in the Belousov-Zhabotinsky reaction," *J. Phys. Chem.* **91**, 501–503.
- Pertsov, A., Vinson, M., and Muller, S. C. (1993). "Three-dimensional reconstruction of organizing centers in excitable chemical media," *Physica D* **72**, 233–240.
- Russ, J. C. (1995). *The Handbook of Image Processing*, 2nd ed. (CRC, Boca Raton, FL).
- Su, S., Menzinger, M., Armstrong, R. L., Cross, A., and Lemaire, C. (1994). "Magnetic resonance imaging of kinematic wave and pacemaker dynamics in the Belousov-Zhabotinsky reaction," *J. Phys. Chem.* **98**, 2494–2498.
- Tyson, J. J. and Keener, J. P. (1994). "A theory of rotating scroll waves in excitable media," in *Chemical Waves and Patterns*, edited by R. Kapral and K. Showalter (Kluwer, Dordrecht), pp. 93–118.
- Tyson, J. J. and Strogatz, S. H. (1991). "The differential geometry of scroll waves," *Int. J. Bifurcation Chaos* **1**, 723–744.
- Tzalmona, A., Armstrong, R. L., Menzinger, M., Cross, A., and Lemaire, C. (1990). "Detection of chemical waves by magnetic resonance imaging," *Chem. Phys. Lett.* **174**, 199–202.
- Vinson, M., Pertsov, A., and Jalife, J. (1993). "Anchoring of vortex filaments in 3D excitable media," *Physica D* **72**, 119–134.
- Welsh, B. J. and Gomati, J. (1990). "Diversity of three-dimensional chemical waves," *Physica D* **43**, 304–317.
- Winfree, A. T. (1974a). "Two kinds of wave in an oscillating chemical solution," *Faraday Symp. Chem. Soc.* **9**, 38–46.
- Winfree, A. T. (1974b). "Rotating solutions to reaction/diffusion equations," in *SIAM/AMS Proceedings 8*, edited by D. Cohen (American Mathematical Society, Providence, RI), pp. 13–21.
- Winfree, A. T. (1985). "Organizing centers for chemical waves in two and three dimensions," in *Oscillations and Traveling Waves in Chemical Systems*, edited by R. J. Field and M. Burger (Wiley, New York), pp. 441–472.
- Winfree, A. T. (1989). "Electrical instability in cardiac muscle: Phase singularities and rotors," *J. Theor. Biol.* **138**, 353–405.
- Winfree, A. T. (1990). "Stable particle-like solutions to nonlinear reaction-diffusion equations," *SIAM Rev.* **32**, 1–53.
- Winfree, A. T. (1992). "Numerical and chemical experiments on filament motion," in *Spatio-temporal Organization in Non-equilibrium systems*, edited by S. C. Muller and T. Plesser (Projekt-Verlag, Dortmund), pp. 270–273.
- Winfree, A. T. (1993). "The geometry of excitability," in *1992 Lectures in Complex Systems*, edited by L. Nadel and D. Stein, SFI Studies in the Sciences of Complexity. V. (Addison-Wesley, Reading, MA), pp. 207–298.
- Winfree, A. T. (1994a). "Lingering mysteries about organizing centers in the Belousov-Zhabotinsky medium and its Oregonator model," in *Chemical Waves and Patterns*, edited by R. Kapral and K. Showalter (Kluwer, Dordrecht), pp. 3–55.
- Winfree, A. T. (1994b). "Persistent tangled vortex rings in generic excitable media," *Nature* **371**, 233–236.
- Winfree, A. T. (1994c). "Electrical turbulence in three-dimensional heart muscle," *Science* **266**, 1003–1006.
- Winfree, A. T. (1995). "Persistent tangles of vortex rings in excitable media," *Physica D* **84**, 126–147.
- Winfree, A. T. and Jahnke, W. (1989). "Three-dimensional scroll ring dynamics in the Belousov-Zhabotinsky reagent and in the 2-variable Oregonator model," *J. Phys. Chem.* **93**, 2823–2832.
- Winfree, A. T. and Strogatz, S. H. (1983a). "Singular filaments organize chemical waves in excitable media. I. Geometrically simple waves," *Physica D* **8**, 35–49.
- Winfree, A. T. and Strogatz, S. H. (1983b). "Singular filaments organize chemical waves in excitable media. II. Twisted waves," *Physica D* **9**, 65–80.
- Winfree, A. T. and Strogatz, S. H. (1983c). "Singular filaments organize chemical waves in excitable media. III. Knotted waves," *Physica D* **9**, 333–345.
- Winfree, A. T. and Strogatz, S. H. (1984a). "Singular filaments organize chemical waves in excitable media. IV. Wave taxonomy," *Physica D* **13**, 221–233.
- Winfree, A. T. and Strogatz, S. H. (1984b). "Organizing centers for three-dimensional chemical waves," *Nature* **311**, 611–615.